Electronic Supplementary Material (ESI) for Journal of Materials Chemistry A.

Supporting Information for

A Metal-Organic Framework Converted Catalyst that Boosts Photo-Electrochemical Water Splitting

Drialys Cardenas-Morcoso,[1,†] *Raya Ifraemov,*[2,†] *Miguel García-Tecedor,*[1] *Itamar Liberman* [2]*Sixto Gimenez,*[1,*] *and Idan Hod,*[2,*]

[1] Institute of Advanced Materials (INAM), Universitat Jaume I, 12071 Castelló, Spain

[2] Department of Chemistry and Ilse Katz Institute for Nanoscale Science and Technology, Ben-Gurion University of the Negev, Beer-Sheva 8410501, Israel

[*]**Email:** sjulia@uji.es, hodi@bgu.ac.il

Experimental

Materials. The chemicals: Bismuth(III) nitrate ($Bi(NO_3)_3{\cdot}5H_2O \geq 98.0\%$), Vanadyl acetylacetonate ($VO(acac)_2 \geq 97.0\%$), potassium phosphate monobasic and dibasic ($KH_2PO_4 \geq 99.0\%$ and $K_2HPO_4 \geq 98.0\%$), zirconyl chloride octahydrate ($ZrOCl_2{\cdot}8H_2O \geq 98.0\%$), Benzene-1,3,5-tricarboxylic acid ($H_3BTC \geq 95\%$), 2-methylimidazole ($C_4H_6N_2 \geq 99\%$), and cobalt nitrate hexahydrate ($Co(NO_3)_2{\cdot}6H_2O \geq 98\%$) were purchased from Sigma-Aldrich. Na_2SO_3 from J.T. Baker, potassium ferri(III)cyanide ($K_3[Fe(CN)_6] \geq 99.5\%$) from fluorochem and potassium chloride ($KCl \geq 99.0\%$)from Frutarom LTD. The Solvents; dimethyl sulfoxide (DMSO ≥ 99.9%), ethylene glycol (ethane-1,2-diol ≥ 99.0%) were obtained from Sigma-Aldrich and Methanol (absolute) from Bio-Lab ltd.

Synthesis of FTO-$BiVO_4$ electrodes.

Zr doped $BiVO_4$ films were prepared through a previously reported method[1] based on the electrodeposition of metallic Bi on fluorine doped tin oxide (FTO) coated glass, followed by a reaction with a vanadium precursor, $VO(acac)_2$ (Sigma-Aldrich) in DMSO, at 450 ºC for 2h. Zr was added as 2.5 mol.% of $ZrCl_2O{\cdot}8H_2O$ (Sigma-Aldrich) to the Bi^{3+} plating bath, according to a previous optimization process.[2]

Modification of $BiVO_4$ electrodes with a ZIF-67.

$BiVO_4$ modified FTO slides (FTO-$BiVO_4$) were immersed (with the conductive side upwards) in a 20 ml methanol solution of H_3BTC (21.01 mg, 5 mM) for 12 hours at room temperature for a surface modification with a monolayer of H_3BTC. The H_3BTC-modified $BiVO_4$ slides were carefully rinsed in methanol and dried in room temperature. Direct growth of ZIF-67 thin films on $BiVO_4$ slides was achieved by immersing the modified slides in a mixture of the two following solutions: 10 ml of $Co(NO_3)_2{\cdot}6H_2O$ (58.21 mg, 20 mM) and 10 ml of 2-methylimidazole (32.84 mg, 40 mM) both in methanol, for different periods of time: 1, 4, 6, 8.5 and 12 hours at room temperature. Thereafter, samples were rinsed gently in methanol for several times and dried in room temperature.

Preparation of $BiVO_4$-CoO_x electrodes.

ZIF-67 modified FTO-$BiVO_4$ samples (1, 4, 6, 8.5 and 12 hours of the MOF synthesis) were heated to 400 ºC in air, at a heating rate of 5 ºC /min. Upon reaching 400 ºC, the temperature was kept constant for 3 hours, and then the samples were cooled-down to room temperature.

Materials Characterization.

The crystalline structure of FTO- $BiVO_4$, $BiVO_4$-ZIF-67 and $BiVO_4$-CoO_x samples before and after calcination in air was confirmed by X-ray diffraction (XRD) measurements on a PANalytical's Empyrean multi-purpose diffractometer, using Cu-Ka (0.15405 nm) radiation. The vibrational modes of the samples were studied by Raman spectroscopy, using a Jobin-Yvon LabRam HR-high resolution analytical Raman instrument equipped with an Argon laser at 514.5 nm as excitation sources, in order to confirm the formation of the metal oxide composite on top of the $BiVO_4$ surface after calcination. Scanning electron microscopy (SEM) images were recorded using a JSM-7499F ultrahigh resolution cold FEG-SEM scanning electron microscope, operating at an acceleration voltage of 3 V with an INCA 400 Oxford EDS analyzer (Oxford, U.K.) in order to observe the morphology, particle size and chemical composition of the samples. EDS-scanning transmission electron microscope (STEM) was utilized for element mapping using annular dark-field imaging method.

N_2 physisorption isotherms for the calcinated ZIF-67 MOF powder were taken at 77 K using a Quantachrome Novatouch porosimeter. The sample was degassed at 120 °C in vacuum for 17 hours prior to isotherm measurement. The surface area of the sample was calculated by applying the Brunauer-Emmett-Teller (BET) model to the isotherm data points (adsorption branch). In order to obtain information about surface structure and possible changes of electronic coordination before and after electrochemical treatment the samples were analyzed by X-ray Photoelectron Spectroscopy (XPS). XPS data were collected by using an X-ray photoelectron spectrometer ESCALAB 250 ultrahigh vacuum (1×10-9 bar) apparatus with an AlKα X-ray source and a monochromator. The X-ray beam size was 500 μm and survey spectra was recorded with a pass energy (PE) of 150 eV and high energy resolution spectra were recorded with a PE of 20 eV. To correct for charging effects, all spectra were calibrated relative to a carbon C 1s peak, positioned at 284.8 eV. XPS results were processed by using the AVANTGE software.

The optical properties of the prepared films were determined through UV-Vis spectrophotometry, using a Cary 300 Bio spectrophotometer. The absorbance (A) was estimated from transmittance (T) and diffuse reflectance (R) measurements as: $A = -\log(T + R)$. The direct optical bandgap of $BiVO_4$ (E_g) was estimated by Tauc plots as: $(h\upsilon\alpha)^{1/n} = A(h\upsilon - E_g)$, where n=1/2 for direct transitions, *h* is the Planck's constant and υ the frequency.

Photo-electrochemical Characterization

The photoelectrochemical performance of the electrodes was evaluated in a three-electrode cell consisting of a working electrode, an Ag/AgCl (3 M KCl) reference electrode, a Pt wire as a counter electrode and a 0.1 M potassium phosphate (K-Pi) buffer solution of pH 7.5 as electrolyte. Alternatively, a 0.1M Na_2SO_3 solution was added to the electrolyte as hole scavenger. The measurements were carried out by using an Autolab potentiostat/galvanostat PGSTAT302, and a 300 W Xe lamp was used for those experiments under illumination conditions. The light intensity was adjusted to 100 mW/cm^2 using a thermopile and illumination was carried out through the FTO substrate. All the potentials were referred to the Reversible Hydrogen Electrode (RHE) through the Nernst equation: $V_{RHE} = V_{Ag/AgCl} + V^{0}_{Ag/AgCl} + 0.059 \cdot pH$. Electrochemical Impedance Spectroscopy (EIS) measurements were performed between 0.1 Hz and 40 kHz with 20 mV of amplitude perturbation, with a step potential of 64 mV in the anodic direction. The EIS data were analyzed with ZView software (Scribner associates). Incident Photon to Current Efficiency (IPCE) measurements were performed with a 300 W Xe lamp coupled with a monochromator and an optical power meter. The photocurrent was measured at 1.23 V vs RHE, with 10 nm spectral step. IPCE was calculated through the expression: $IPCE\,\% = \frac{I_{ph}(A)}{P(W)} \times \frac{1239.8}{\lambda\,(nm)} \times 100$, where I_{ph} is the photocurrent measured at a wavelength λ and *P* is the power of the monochromatic light at the same wavelength. The Absorbed Photon to Current Efficiency (APCE) was also calculated as: $APCE\,\% = \frac{IPCE}{\eta_{e^-/h^+}} \times 100$, where η_{e^-/h^+} is the absorptance, defined as the fraction of electron–hole pairs generated per incident photon flux and was obtained from the absorbance (A) as $\eta_{e^-/h^+} = 1 - 10^{-A}$. From measurements in the presence of a Na_2SO_3 sacrificial hole scavenger and the theoretical maximum photocurrent estimated from the absorbance measurements, ($j_{abs} = \frac{e}{hc}\int \lambda \cdot I(\lambda) \cdot (1 - 10^{-A})\,d\lambda$, with *I(λ)*as the spectral irradiance, *e* the elemental charge, *h* the Planck constant and *c* the light speed), the charge separation efficiency (η_{cs}) and the charge injection efficiency (η_{cat}) were calculated as: $\eta_{cat} = \frac{j_{H_2O}}{j_{HS}}$ and $\eta_{cs} = \frac{j_{HS}}{j_{abs}}$. The faradaic efficiency for O_2 evolution at the electrode surface was estimated through the relation between the amount of evolved O_2 monitored every 5 min during a measurement at 1.23 V vs RHE in phosphate buffer (pH 7.5), in a sealed cell coupled to an Agilent Micro-GC gas chromatograph, and the theoretical O_2 evolution calculated with the Faraday´s Law.

Scanning electrochemical microscopy (SECM) measurements were performed on the $BiVO_4$ (400 °C) and the $BiVO_4$-CoO_x_6h electrodes, utilizing a BIOLOGIC SECM-150 workstation. The measurements were performed in a phosphate buffer solution (pH=7.5), were the $BiVO_4$-based films function as the substrate, a Pt ultramicroelectrode (UME) with radius of 5 μm utilized as the SECM tip, while Ag/AgCl (St.) and Pt wire were served as the reference and the counter electrode, respectively. In the SECM substrate-generation tip-collection measurements, the potential on the tip was kept constant at 0.1 V_{RHE} while the potential on substrate was swept from 0.65 V_{RHE} to 1.7 V_{RHE} with a scan rate of 5 mV/sec. The measurements were performed under light illumination using a 2 mW/cm^2 405 nm LED lamp. Prior to the measurement the gap spacing (Z), between the tip and a substrate was determined by monitoring the tip position, using an aqueous solution containing 5 mM ferricyanide and 0.1 M KCl, while keeping the tip and substrate in a constant potential of 0.4 V and 1.2 V vs RHE. The obtained approach curves where fitted with using a MIRA SECM simulation software to accurately extract the substrate-to-tip distance.

Supplementary Results.

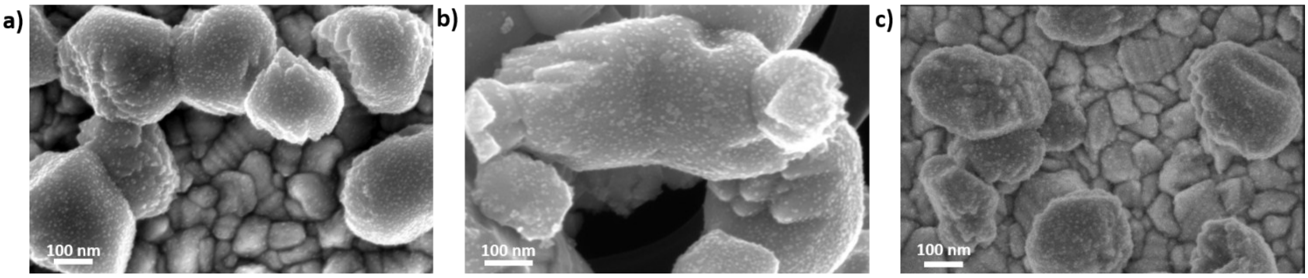

Figure S1. SEM images of a) $BiVO_4$-CoO_x_6h, b) $BiVO_4$-CoO_x_8.5h, and c) $BiVO_4$-CoO_x_12h.

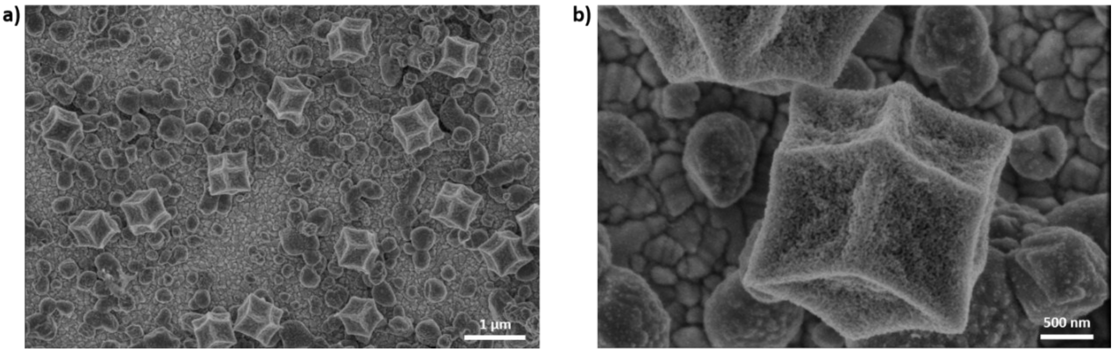

Figure S2. SEM image of dodecahedral ZIF-67-converted CoO_x particles in $BiVO_4$-CoO_x_6h films.

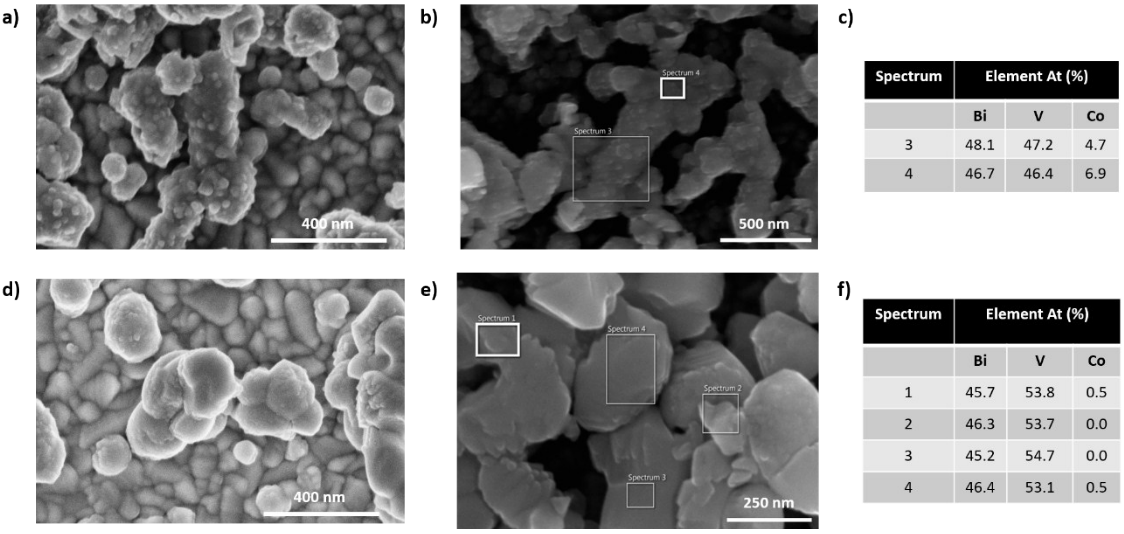

Spectrum	Element At (%)		
	Bi	V	Co
3	48.1	47.2	4.7
4	46.7	46.4	6.9

Spectrum	Element At (%)		
	Bi	V	Co
1	45.7	53.8	0.5
2	46.3	53.7	0.0
3	45.2	54.7	0.0
4	46.4	53.1	0.5

Figure S3. SEM images, EDS atomic percentage of the selected elements and their corresponding regions in SEM of the $BiVO_4$-ZIF-67_6h (a-c) and $BiVO_4$-$Co(NO_3)_2$_6h (d-f).

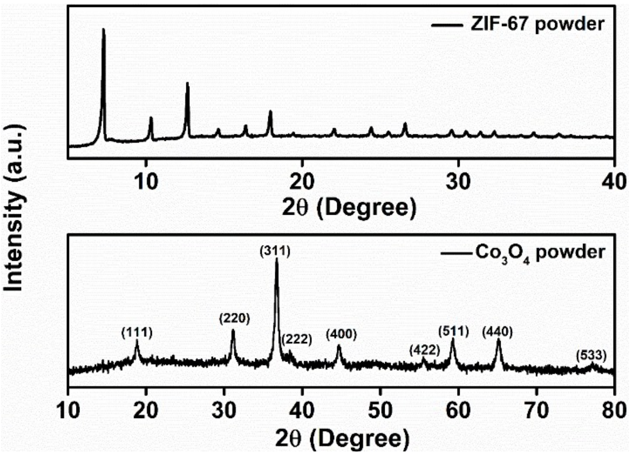

Figure S4. PXRD patterns of as synthesized ZIF-67 powder (top) and ZIF-67 converted Co_3O_4 (bottom).

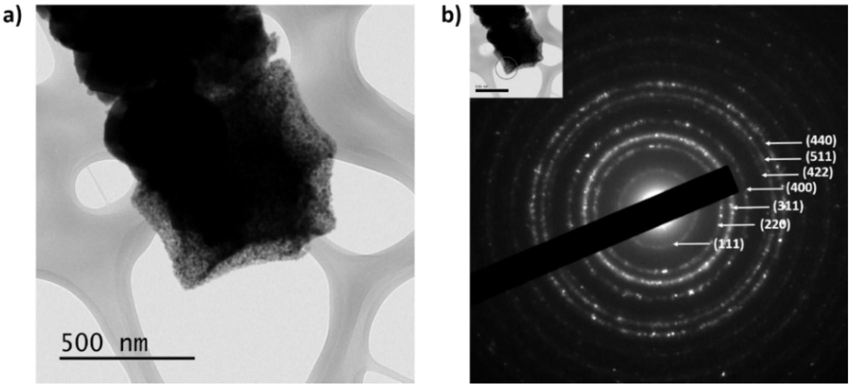

Figure S5. a) Transmission electron microscopy (TEM) images of ZIF-67 converted porous CoO_x, b) Selected area electron diffraction (SAED) of CoO_x exhibiting diffraction rings corresponding to a cubic Co_3O_4 crystal phase.

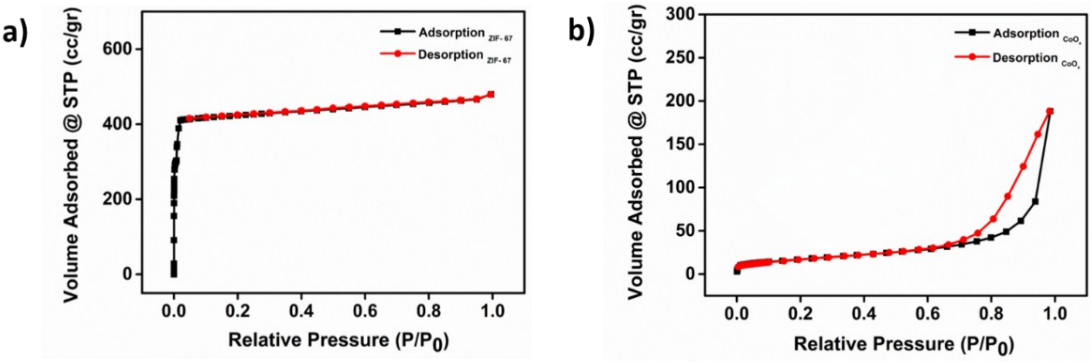

Figure S6. N_2 isotherm analysis of a) as-synthesized ZIF-67 (BET surface area of 1340 m^2/g), and b) air calcinated ZIF-67 (CoO_x) powder (BET surface area of 63 m^2/g).

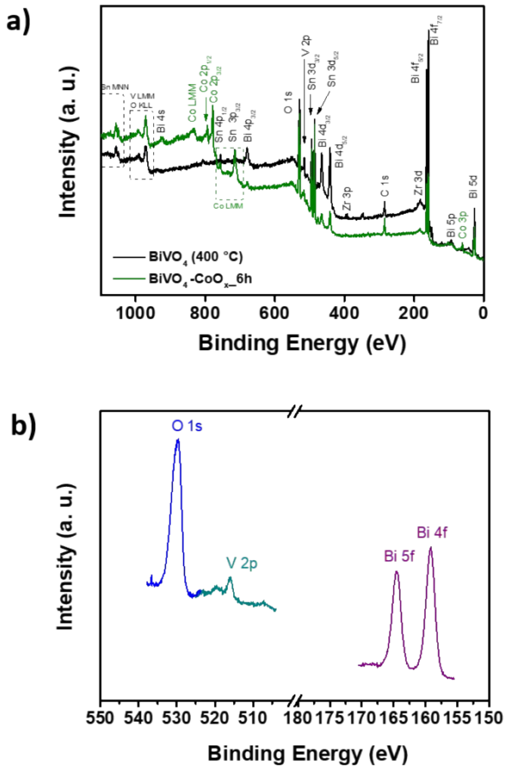

Figure S7. (a) Global XPS spectra of $BiVO_4$ (400 ºC, control) and $BiVO_4$-CoOx_6h electrodes surface. (b) XPS spectra of specific O 1s, V 2p and Bi 4f orbitals in $BiVO_4$-CoOx_6h electrode surface.

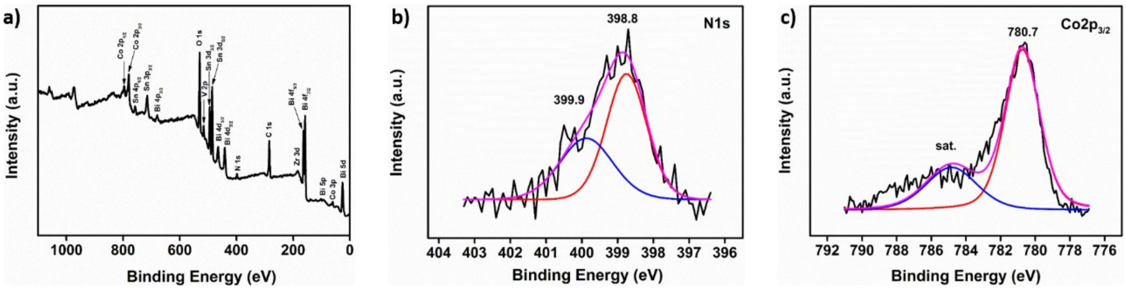

Figure S8. a) Global, b) N1s and c) Co2p XPS spectra of $BiVO_4$-ZIF-67_6h sample

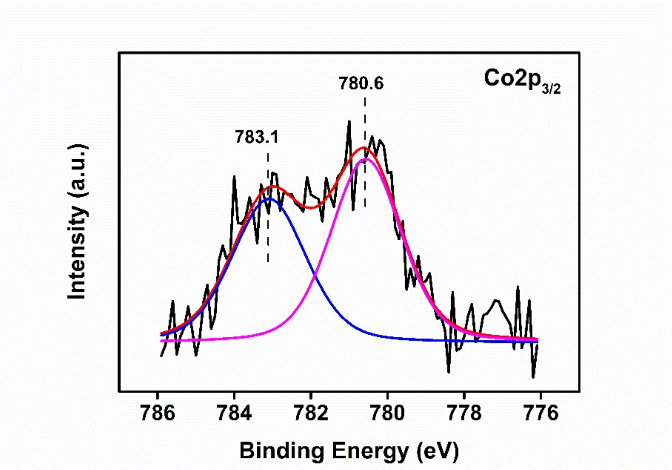

Figure S9. XPS Spectra analysis of the signals of Co 2p orbitals in $BiVO_4$-CoO_x_6h films, showing the presence of both CoO_x and Co_3O_4 surface-residing phases.

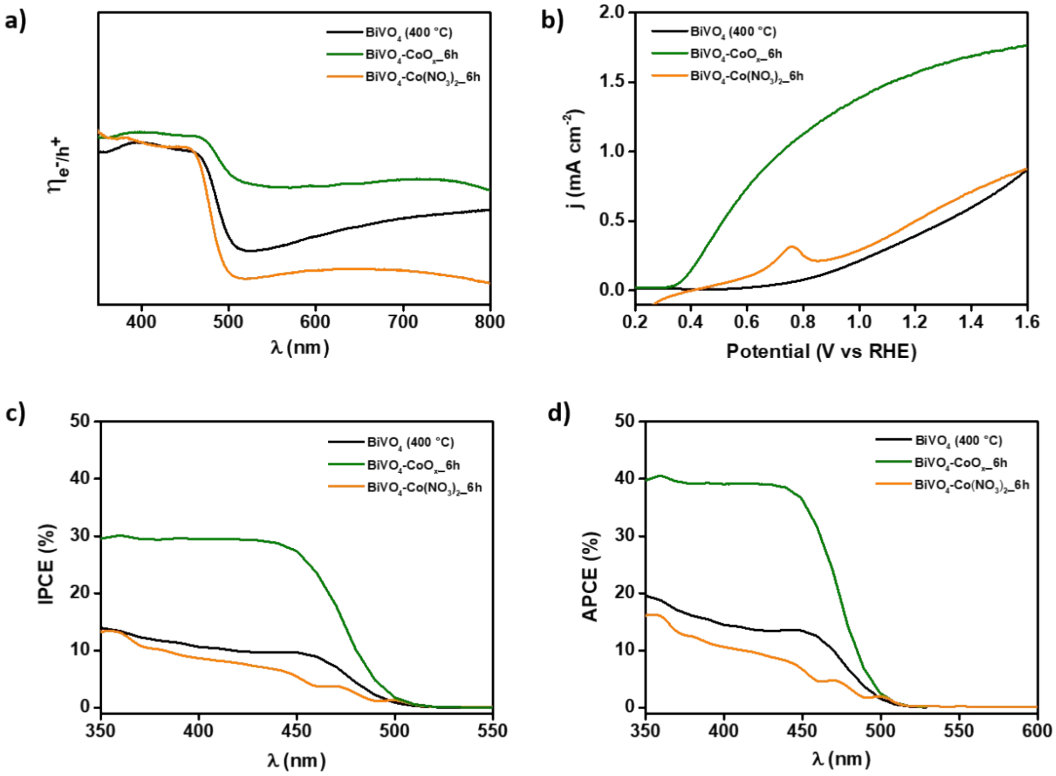

Figure S10. a) UV-Vis absorption spectra of the two control sample: $BiVO_4$ (400 °C) , $BiVO_4$_$Co(NO_3)_2$ and the $BiVO_4$-CoO_x_6h, b) j-V curves obtained with cyclic voltammetry c) IPCE and d) APCE spectra obtained from IPCE and absorbance measurements at 1.23 V vs RHE

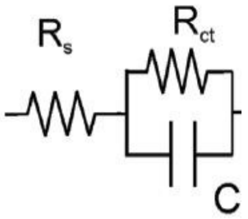

Figure S11. Equivalent circuit model used to fit the experimental EIS data. The circuit includes a series resistance (R_s) accounting for the solution resistance and the resistance at the contacts, a charge transfer resistance (R_{ct}) accounting for the injection of carriers (holes) into the solution, and a capacitance (C).

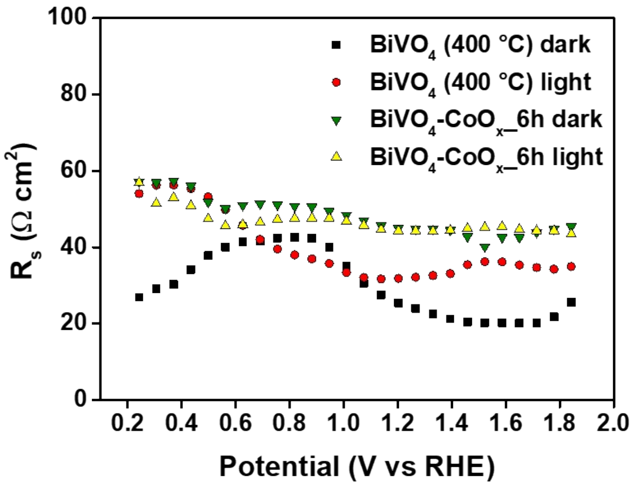

Figure S12. Series resistance (R_s) of the $BiVO_4$ (400 °C) and best performing $BiVO_4$-CoO_x_6h electrode in the dark and under illumination at 100 mW·cm^{-2}.

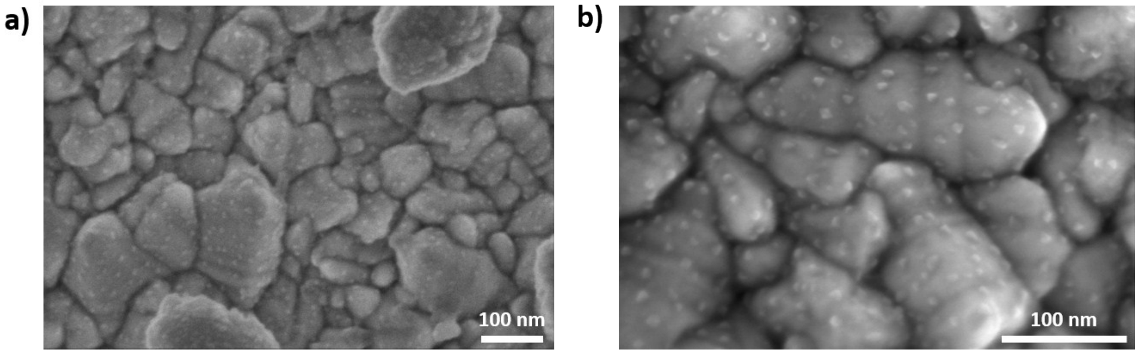

Figure S13. SEM images of the FTO/CoO_x interface at an $BiVO_4$-CoO_x_6h electrode.

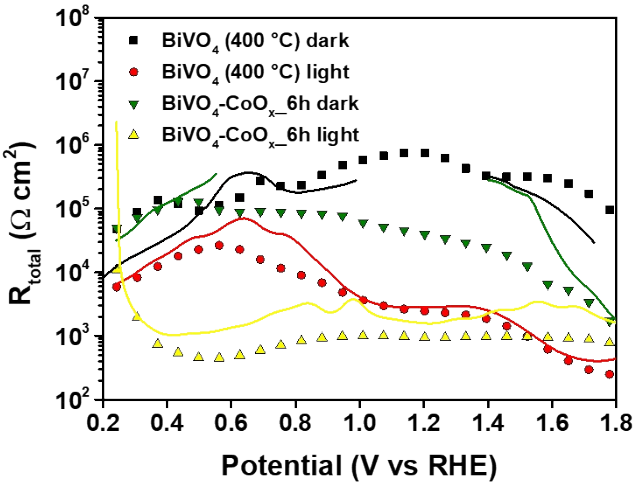

Figure S14. Comparison between the total resistance (R_{total}) extracted from impedance spectroscopy and from derivation of the j-V curves obtained by cyclic voltammetry,

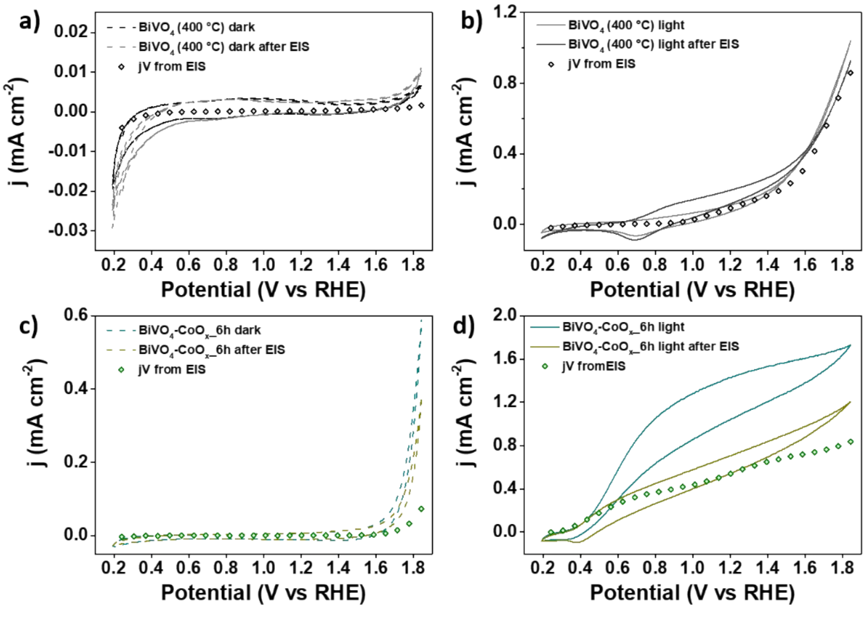

Figure S15. Cyclic voltammetry j-V curves before and after the impedance spectroscopy measurements (lines) together with j-V curves directly extracted from impedance measurements.

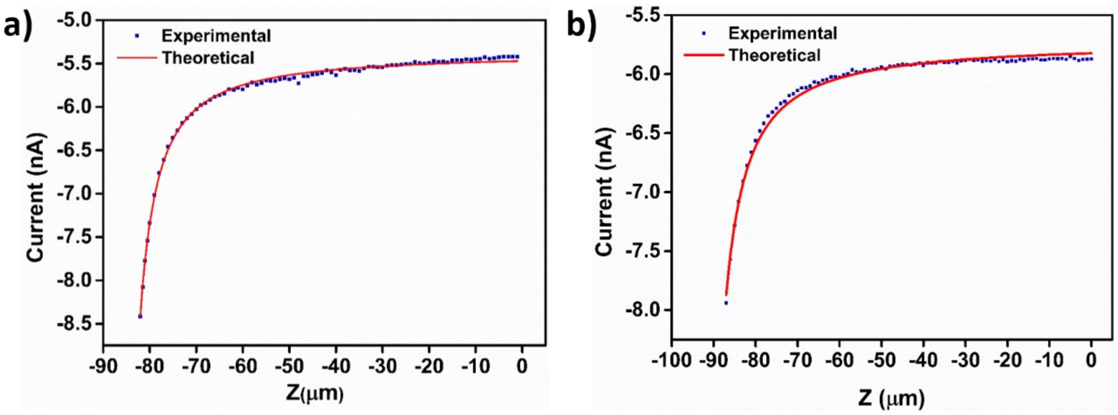

Figure S16. SECM approach curves for the (a) $BiVO_4$ (400 °C) and, (b) $BiVO_4$-CoO_x_6h electrodes. The measurement was performed in an aqueous solution containing 5 mM ferricyanide, 0.1 M KCl, while the potential on the tip and substrate held at 0.4 V and 1.2 V vs RHE, respectively. The experimental results (blue dots) are compared to the theoretical approach curves obtained from MIRA Simulation software (red line).

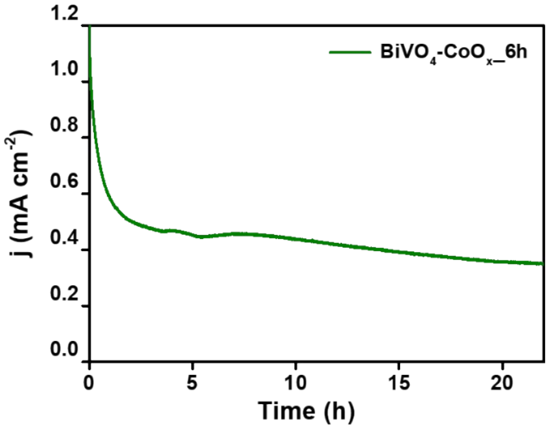

Figure S17. Long term stability in $BiVO_4$-CoO_x_6h electrode.

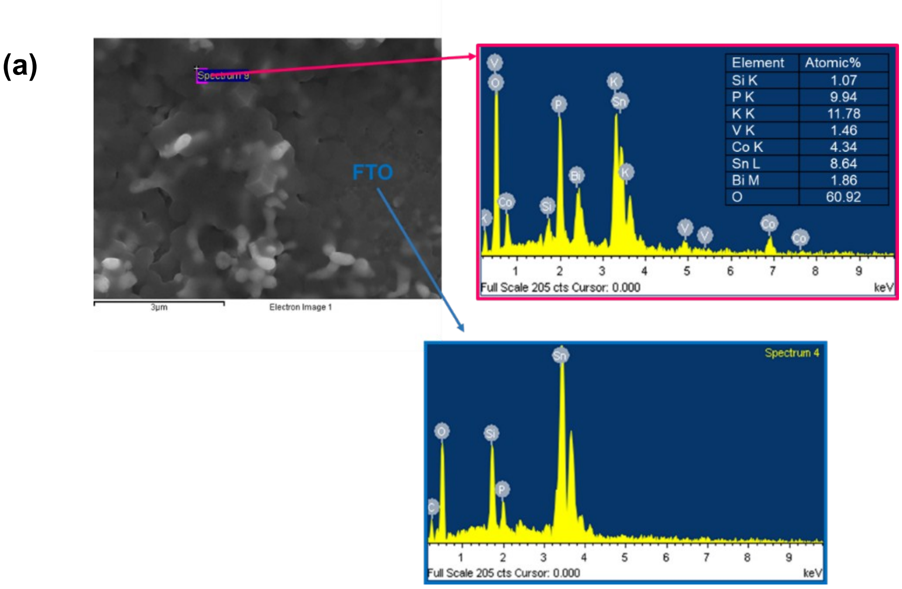

Element	Atomic%
Si K	1.07
P K	9.94
K K	11.78
V K	1.46
Co K	4.34
Sn L	8.64
Bi M	1.86
O	60.92

Figure S18. Post-mortem (a) SEM and (b) XPS analysis on $BiVO_4$-CoO_x_6h electrode surface after long term stability test.

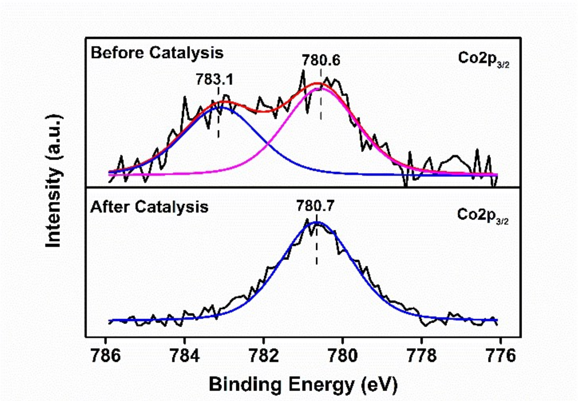

Figure S19. XPS spectra of $BiVO_4$-CoO_x_6h before and after long term stability measurement.

Table S1: ICP analysis for Co surface loading for the 6, 8.5, 12 hours ZIF-67 growth duration.

Sample	Co (µg/cm^2)	Co (µmol/cm^2)
ZIF-67_6h	9.778	0.166
ZIF-67_8.5h	16.60	0.282
ZIF-67_12h	35.85	0.608

Table S2. Comparison of current density values extracted from j-V curves and calculated from IPCE measurements at 1.23 V vs RHE.

Sample	*j @1.23 V vs RHE from jV (mA cm^{-2})*	*j from IPCE (mA cm^{-2}) [300 nm-540 nm]*
$BiVO_4$ 400ºC (control)	0.428	0.666
$BiVO_4$-CoO_x_1h	0.538	0.523
$BiVO_4$-CoO_x_4h	0.781	0.704
$BiVO_4$-CoO_x_6h	1.59	1.654
$BiVO_4$-CoO_x_8.5h	1.33	1.468
$BiVO_4$-CoO_x_12h	1.16	1.179

Table S3. ICP-MS elemental analysis of the electrolyte after long term stability test of $BiVO_4$-CoO_x_6h electrode. (Analysis performed in an Agilent 7500cx quadrupole analyzer equipped with collision cell)

Element	**Before stability test**	**After stability test**
	[X] in ppb (µg/L)	
V	0.94	16.9
Co	0.06	19.5
Bi	0.43	7.68

Table S4. Elemental quantification for XPS analysis on $BiVO_4$-CoO_x_6h electrode surface before and after long term stability test.

	Atomic %	
Element	**$BiVO_4$/ZIF-67, 6h**	**$BiVO_4$/ZIF-67, 6h Aged**
O	48.2	41.7
Sn	7.7	-
N	3.1	-
Ca	-	-
C	23.3	20.5
Bi	4.3	0.3
V	2.7	-

Co	10.6	1.2
K	-	23.6
P	-	12.7

References:

1. D. Kang, Y. Park, J. C. Hill and K.-S. Choi, *J. Phys. Chem. Lett.*, 2014, 5, 2994-2999.
2. T. W. Kim and K.-S. Choi, *Science*, 2014, 343, 990-994.